Since January 2020 Elsevier has created a COVID-19 resource centre with free information in English and Mandarin on the novel coronavirus COVID-19. The COVID-19 resource centre is hosted on Elsevier Connect, the company's public news and information website.

Results in Physics 21 (2021) 103776

Contents lists available at ScienceDirect

Results in Physics

journal homepage: www.elsevier.com/locate/rinp

A mathematical model of Coronavirus Disease (COVID-19) containing asymptomatic and symptomatic classes☆

Idris Ahmed [a,b], Goni Umar Modu [c], Abdullahi Yusuf [d,e], Poom Kumam [b,f,*], Ibrahim Yusuf [g]

[a] Department of Mathematics, Faculty of Science, King Mongkut's University of Technology Thonburi (KMUTT), 126 Pracha-Uthit Road, Bang Mod, Thung Khru, Bangkok 10140, Thailand
[b] KMUTTFixed Point Research Laboratory, Fixed Point Theory and Applications Research Group, Center of Excellence in Theoretical and Computational Science (TaCS-CoE), Faculty of Science, King Mongkut's University of Technology Thonburi (KMUTT), 126 Pracha-Uthit Road, Bang Mod, Thung Khru, Bangkok 10140, Thailand
[c] Department of Statistics, Ramat Polytechnic Maiduguri, P. M. B 1070 Maiduguri, Borno State, Nigeria
[d] Department of Computer Engineering, Biruni University, Istanbul 34010, Turkey
[e] Department of Mathematics, Federal University Dutse, Jigawa 7156, Nigeria
[f] Department of Medical Research, China Medical University Hospital, China Medical University, Taichung 40402, Taiwan
[g] Department of Mathematical Sciences, Bayero University Kano, P. M. B. 3011 Kano, Nigeria

ARTICLE INFO

Keywords:
Corona virus
Basic reproductive number
Nonlinear differential equations
ABC-fractional operator
Mathematical model
Existence and uniqueness
Sensitivity analysis

2010 MSC:
47H10
34A12
39A30

ABSTRACT

The research work in this paper attempts to describe the outbreak of Coronavirus Disease 2019 (COVID-19) with the help of a mathematical model using both the Ordinary Differential Equation (ODE) and Fractional Differential Equation. The spread of the disease has been on the increase across the globe for some time with no end in sight. The research used the data of COVID-19 cases in Nigeria for the numerical simulation which has been fitted to the model. We brought in the consideration of both asymptomatic and symptomatic infected individuals with the fact that an exposed individual is either sent to quarantine first or move to one of the infected classes with the possibility that susceptible individual can also move to quarantined class directly. It was found that the proposed model has two equilibrium points; the disease-free equilibrium point (DFE) and the endemic equilibrium point (E_1). Stability analysis of the equilibrium points shows (E_0) is locally asymptotically stable whenever the basic reproduction number, $\mathscr{R}_0 < 1$ and (E_1) is globally asymptotically stable whenever $\mathscr{R}_0 > 1$. Sensitivity analysis of the parameters in the $\mathscr{R}_0$ was conducted and the profile of each state variable was also depicted using the fitted values of the parameters showing the spread of the disease. The most sensitive parameters in the $\mathscr{R}_0$ are the contact rate between susceptible individuals and the rate of transfer of individuals from exposed class to symptomatically infected class. Moreover, the basic reproduction number for the data is calculated as $\mathscr{R}_0 \approx 1.7031$. Existence and uniqueness of solution established via the technique of fixed point theorem. Also, using the least square curve fitting method together with the *fminsearch* function in the **MATLAB** optimization toolbox, we obtain the best values for some of the unknown biological parameters involved in the proposed model. Furthermore, we solved the fractional model numerically using the Atangana-Toufik numerical scheme and presenting different forms of graphical results that can be useful in minimizing the infection.

1. Introduction

A mathematical model is a description of the workings of the real world employing mathematical symbols, equations, and formulas. Mathematical models are commonly used in many fields, such as medicine [39], agriculture [25,47], management and social sciences [41] and references cited therein. Such models can either be linear or nonlinear, stochastic or deterministic. In the health sector,

☆ This project was supported by the Petchra Pra Jom Klao Doctoral Scholarship for Ph.D. program of King Mongkut's University of Technology Thonburi (KMUTT). The Center of Excellence in Theoretical and Computational Science (TaCS-CoE), KMUTT.

* Corresponding author at: KMUTTFixed Point Research Laboratory, Fixed Point Theory and Applications Research Group, Center of Excellence in Theoretical and Computational Science (TaCS-CoE), Faculty of Science, King Mongkut's University of Technology Thonburi (KMUTT), 126 Pracha-Uthit Road, Bang Mod, Thung Khru, Bangkok 10140, Thailand.
E-mail addresses: goni.umar@ramatpoly.edu.ng (G.U. Modu), yusufabdullahi@fud.edu.ng (A. Yusuf), poom.kum@kmutt.ac.th (P. Kumam), iyusuf.cs@buk.edu.ng (I. Yusuf).

https://doi.org/10.1016/j.rinp.2020.103776
Received 20 October 2020; Received in revised form 11 December 2020; Accepted 16 December 2020
Available online 6 January 2021

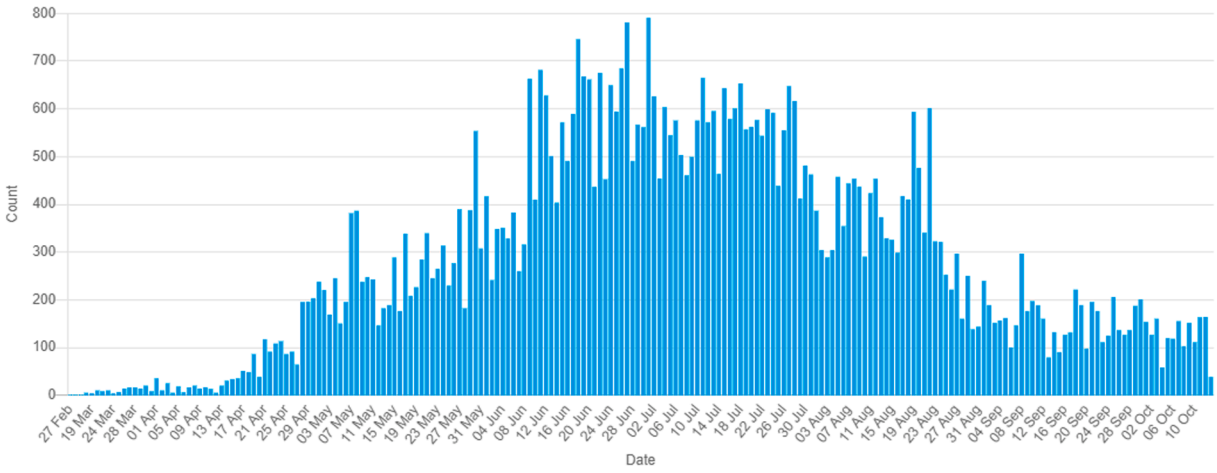

Fig. 1.1. Confirmed COVID-19 Cases-Nigeria 2020 [1].

mathematical models have been used to forecast disease outbreaks, avoid or cure these illnesses. Currently, there are many mathematical models used to explain disease processes and they can be found in books dedicated to mathematical models in biology and medicine, for more details, refer the reader to [10,18,26,35]. By the end of December 2019, the world's deadly coronavirus pandemic, popularly known as COVID-19, erupted in the ancient town of Wuhan Hubei Province, China spreading almost through several countries in 2020 [2]. Several unexplained cases of cough, pneumonia, dyspnea, exhaustion and there were fever in Wuhan, China, for a short period. The arrival of COVID-19 resulted in the closure of business, schools, markets, traveling within and outside, intermingle, curfew, lockdown, reduction of gathering to mention but a few [3].

Nigeria has fallen into the category of nations affected by the coronavirus pandemic. February 27, 2020, culminated in the arrival of the pioneer case of COVID-19 in Lagos state southwestern Nigeria when an Italian citizen arrived on 24 February and presented at a health facility on 26 February 2020 (see Fig. 1.1) [1]. Before the arrival of COVID-19 into Nigeria, the Federal government with some states in Nigeria established various medical agencies and isolation centers to handle and stop the spread of the pandemic. The Federal government through its Nigeria Center for Disease Control (NCDC) provide appropriate public health advice to Nigerians, on the symptoms, dissemination, and prevention of information with national and sub-national networks of public health staff, built capacity for contact tracing and case management and strengthened some laboratories for diagnostic activities of the pandemic.

With the arrival of COVID-19, researchers have been using and formulating mathematical models as a technique in gaining insight into the mode of spread of the pandemic, transmission, impact of the pandemic, prevention and control of the pandemic, the influence of preventive measure on the pandemic ranging from washing hands with a disinfectant such as a hand sanitizer, 2 to 5 meters social distance and use of face mask, see the recent literature [20,33,34,36,43,48,50,53–55]. Okuonghae and Omame [38] analyzed the spread and behavior of COVID-19 in Lagos, Nigeria. Roseline et al. [37] used the linear regression method to modeled the rate of fatality of the pandemic in Nigeria. Adegboye et al. [6] dealt with early spread of COVID-19 in Nigeria. Ajisegiri et al. [9] analyzed the outbreak scenario of COVID-19 in Nigeria. Researchers in different areas have presented excellent research on preventive and curative steps to contain the pandemic and have reported better outcomes. However, a further review of the latest form of models with a justified and satisfactory evaluation is required.

In all of the research cited above, the models presented therein were based On classical derivatives with some restrictions on the order of differential equations involved. To overcome these limitations, several researchers have sought the aid of a rapidly growing field of mathematics known as fractional calculus. The differential operators used in fractional calculus are non-integer or fractional order, which have memory features and are useful in demonstrating many natural phenomena and facts having non-local dynamics behavior. The concept of fractional order has gained significant attention due to its wide-ranging advances and various applications in knowledge areas, see [13,14,21,22,32,40]. Recently, Atangana and Baleanu [16] proposed a new fractional derivative operator with a nonsingular and Mittag-Leffer kernel. The main advantage of the operator is that it has a nonlocal and nonsingular kernel. More recently, new advances and studies in fractional differential equations has been published from a mathematical modeling point of view, see recent papers [4,7,8,11,12,15,19,27–30,44,46,52].

The paper is organized as follows: In Section 2, we formulated the model together with the description of the parameters defined in the model. In Section 3, we obtain the invariant region. Also, we compute the basic reproduction number and study it is disease-free equilibrium (DFE), local stability, the existence of endemic equilibrium, local stability of the endemic equilibrium, and global stability of the endemic equilibrium. The existence and uniqueness of solutions were investigated via the techniques of fixed point theorems in Section 4. In Section 5, we present the model fitting as well as the estimation of the parameters. Besides, sensitivity analysis and numerical simulation are also highlighted. Finally, we give the conclusion of the paper in Section 6.

2. Model formulation

In this research paper, a model of the coronavirus (COVID-19) disease using simple rates of transmission is considered. Let $N(t)$ be the total population of human. This population is divided into seven classes: susceptible individuals $S(t)$, exposed individuals $E(t)$, asymptotically infected individuals $I_A(t)$, symptomatic infected individuals $I_S(t)$, quarantined individuals $Q(t)$, and individuals that have recovered/remove from COVID-19 $R(t)$. Based on this consideration, the total population is $N(t) = S(t) + E(t) + Q(t) + I_A(t) + I_S(t) + R(t)$.

The natural human natality and mortality rates are denoted by Λ and μ respectively. Susceptible individuals (S) gets infected from enough contact with exposed individuals (E) at the rate of β or just move to quarantined class at the rate of τ. The exposed individuals (E) may move to quarantined (Q) class first or get infected without symptoms (asymptomatic) (I_A) or with symptoms (symptomatic) (I_S) at the rates of γ, σ and η respectively. Also quarantined individuals (Q) may be confirmed infected through a test with symptoms (I_S) or without symptoms (I_A) at the rates of υ and θ respectively. The asymptomatic infected individuals (I_A) may recover at the rate of r_1 and the symptomatic infected individuals (I_S) at the rate of r_2.

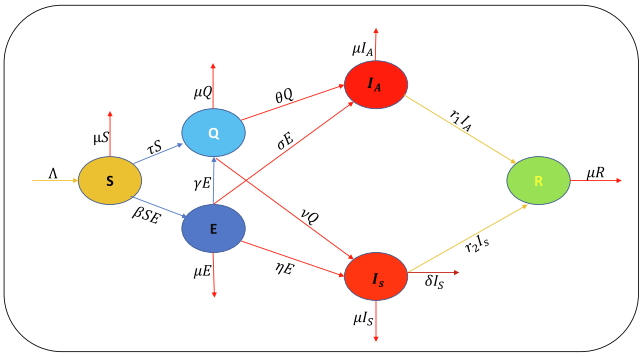

Fig. 2.2. Transmission pattern of COVID-19.

Table 1
Notations used and their meaning.

Parameter	Description
τ	Transfer rate from susceptible individuals to quarantine
β	Contact rate between susceptible individuals and exposed individuals
δ	Mortality rate due to coronavirus in symptomatic infected individual class
γ	Rate of transfer of exposed individuals to quarantine
η	Rate of transfer of individuals from exposed class to symptomatic infected individuals class
θ	Rate of quarantined individuals to asymptomatic infected individuals class
μ	Natural mortality rate
υ	Rate of transfer of quarantined individuals to symptomatic infected individuals class
σ	Rate of transfer of exposed individuals to asymptomatic individuals class
Λ	Recruitment (natality) rate
r_1	Recovery rate of asymptomatic infected individuals
r_2	Recovery rate of symptomatic infected individuals

Each of these classes may decrease as a result of natural mortality μ, while the class of individuals infected with symptoms (I_S) may also decrease as a result of death from the disease at the rate of δ. In the infected class of individuals without symptoms (I_A), the death as a result of the disease is not considered. The possibility of reinfection after recovery has not been considered in this model.

Fig. 2.2, below depicted the schematic diagram showing the spread of COVID-19. Through the schematic diagram depicted in Fig. 2.2, a system of nonlinear differential equations is obtained and presented below (see Table 1):

$$\begin{aligned}
\frac{dS(t)}{dt} &= \Lambda - (\tau+\mu)S(t) - \beta S(t)E(t),\\
\frac{dE(t)}{dt} &= \beta S(t)E(t) - (\gamma+\mu+\eta+\sigma)E(t),\\
\frac{dQ(t)}{dt} &= \tau S(t) + \gamma E(t) - (\mu+\upsilon+\theta)Q(t),\\
\frac{dI_A(t)}{dt} &= \sigma E(t) + \theta Q(t) - (\mu+r_1)I_A(t),\\
\frac{dI_S(t)}{dt} &= \eta E(t) + \upsilon Q(t) - (\delta+\mu+r_2)I_S(t),\\
\frac{dR(t)}{dt} &= r_1 I_A(t) + r_2 I_S(t) - \mu R(t),
\end{aligned} \tag{2.1}$$

subject to the following initial conditions:

$$\begin{aligned}
&S(0)\geq 0, \quad E(0)\geq 0, \quad Q(0)\geq 0, \quad I_A(0)\geq 0,\\
&I_S(0)\geq 0, \quad R(0)\geq 0.
\end{aligned} \tag{2.2}$$

3. Qualitative analysis of the proposed model

Reproduction number is vital in the study of infection disease model [23]. This section presents the computation and presentation of basic reproduction number and invariant region for the proposed model (2.1) and study the

- Locally asymptotically stability of its disease free equilibrium (see Theorem 3.1).
- Unique endemic equilibrium point (see Theorem 3.2).
- Locally asymptotically stability of its unique endemic equilibrium point (see Theorem 3.3).
- Globally asymptotically stable of its endemic equilibrium (see Theorem 3.5).

3.1. *Invariant region*

Having described the human population in the model (2.1), it is vital to show that the state parameters $S(t), E(t), Q(t), I_A(t), I_S(t), R(t)$ are nonnegative for all $t \geq 0$. Solution with positive initial data remains positive for all $t \geq 0$ and are bounded. It is easy to see from systems (2.1) that $\frac{dN(t)}{dt} = \Lambda - \mu N(t) - \delta I_S(t)$ and $\sup_{t\to+\infty} N(t) \leqslant \frac{\Lambda}{\mu}$. As such we can study the system (2.1) in the following feasible region:

$$\Omega = \left\{ \left(S(t), E(t), Q(t), I_A(t), I_S(t), R(t)\right) \in \mathbb{R}^6_+ : 0 \leqslant N(t) \leqslant \frac{\Lambda}{\mu} \right\}. \tag{3.1}$$

(3.1) is now positive invariant in relation to (2.1). Meaning the proposed model (2.1) is epidemiologically well posed and all solutions of the system with $(S(t), E(t), Q(t), I_A(t), I_S(t), R(t)) \in \mathbb{R}^6_+$ remain in Ω.

3.2. *Disease free equilibrium point* (DFE)

Setting the parameters $E = Q = I_A = I_S = R = 0$, the disease free equilibrium is obtained. Therefore, the system (2.1) indicates that the DFE point is given by

$$DFE = (S_0, 0, 0, 0, 0, 0) = \left(\frac{\Lambda}{\tau+\mu}, 0, 0, 0, 0, 0\right). \tag{3.2}$$

The basic reproduction number denoted by $\mathscr{R}_0$ is the expected value of infection rate per time unit. The infection occurs in a susceptible population, caused by an infected individual. Based on the system (2.1), the article generates an equation that involves the classes of exposed and infected population. The disease reproduction number $\mathscr{R}_0$ of the proposed model (2.1) is defined herein in the infected classes. This threshold quantity has been described in [23,51]. In all cases, $\mathscr{R}_0 < 1$ implies that disease will decline, whereas $\mathscr{R}_0 > 1$ implies that disease will persist within a community and $\mathscr{R}_0 = 1$ requires further investigation. $\mathscr{R}_0$ is obtained using the next generation matrix approach [23] where several authors have used it.

We implore the use of a next-generation matrix to find the basic reproduction number for the model (2.1). Without loss of generality, it is clear from the model (2.1), the article generates an equation that involves the classes of the exposed population, infected population without symptom, and infected population with symptom as follows:

$$\begin{aligned}
\frac{dE(t)}{dt} &= \beta S(t)E(t) - (\gamma+\mu+\eta+\sigma)E(t),\\
\frac{dQ(t)}{dt} &= \tau S(t) + \gamma E(t) - (\mu+\upsilon+\theta)Q(t),\\
\frac{dI_A(t)}{dt} &= \sigma E(t) + \theta Q(t) - (\mu+r_1)I_A(t),\\
\frac{dI_S(t)}{dt} &= \eta E(t) + \upsilon Q(t) - (\delta+\mu+r_2)I_S(t).
\end{aligned} \tag{3.3}$$

Referring to [51], from the equations (3.3), the study generates

matrix $\mathscr{F}$ and $\mathscr{V}$, i.e.

$$\mathscr{F} = \begin{pmatrix} \beta S(t)E(t) \\ 0 \\ 0 \\ 0 \end{pmatrix},$$

and

$$\mathscr{V} = \begin{pmatrix} (\gamma+\mu+\eta+\sigma)E(t) \\ -\tau S(t) - \gamma E(t) + (\mu+\upsilon+\theta)Q(t) \\ -\sigma E(t) - \theta Q(t) + (\mu+r_1)I_A(t) \\ -\eta E(t) - \upsilon Q(t) + (\delta+\mu+r_2)I_S(t) \end{pmatrix}.$$

The Jacobian matrix of $\mathscr{F}$ and $\mathscr{V}$ at DFE, denoted by F and V are given as follows:

$$F = \begin{pmatrix} \frac{\beta\Lambda}{\tau+\mu} & 0 & 0 & 0 \\ 0 & 0 & 0 & 0 \\ 0 & 0 & 0 & 0 \\ 0 & 0 & 0 & 0 \end{pmatrix},$$

$$V = \begin{pmatrix} \gamma+\mu+\eta+\sigma & 0 & 0 & 0 \\ -\gamma & \mu+\upsilon+\theta & 0 & 0 \\ -\sigma & -\theta & \mu+r_1 & 0 \\ -\eta & -\upsilon & 0 & \delta+\mu+r_2 \end{pmatrix}.$$

$$J = \begin{pmatrix} -(\tau+\mu)-\beta E & -\beta S & 0 & 0 & 0 & 0 \\ \beta E & \beta S-(\gamma+\mu+\eta+\sigma) & 0 & 0 & 0 & 0 \\ \tau & \gamma & -(\mu+\upsilon+\theta) & 0 & 0 & 0 \\ 0 & \sigma & \theta & -(\mu+r_1) & 0 & 0 \\ 0 & \eta & \upsilon & 0 & -(\delta+\mu+r_2) & 0 \\ 0 & 0 & 0 & r_1 & r_2 & -\mu \end{pmatrix},$$

which implies

$$J_{DFE} = \begin{pmatrix} -(\tau+\mu) & \frac{-\beta\Lambda}{(\tau+\mu)} & 0 & 0 & 0 & 0 \\ 0 & \frac{\beta\Lambda-(\tau+\mu)(\gamma+\mu+\eta+\sigma)}{\tau+\mu} & 0 & 0 & 0 & 0 \\ \tau & \gamma & -(\mu+\upsilon+\theta) & 0 & 0 & 0 \\ 0 & \sigma & \theta & -(\mu+r_1) & 0 & 0 \\ 0 & \eta & \upsilon & 0 & -(\delta+\mu+r_2) & 0 \\ 0 & 0 & 0 & r_1 & r_2 & -\mu \end{pmatrix}.$$

The characteristic polynomial of the Jacobian matrix at DFE is given by $det(J_{DFE}-\lambda I)= 0$, where λ is the eigenvalue and I is 6×6 identity matrix. Thus, the determinant of $(J_{DFE}-\lambda I)$ is

$$\begin{vmatrix} -(\tau+\mu)-\lambda & \frac{-\beta\Lambda}{(\tau+\mu)} & 0 & 0 & 0 & 0 \\ 0 & \frac{\beta\Lambda-(\tau+\mu)(\gamma+\mu+\eta+\sigma)}{\tau+\mu}-\lambda & 0 & 0 & 0 & 0 \\ \tau & \gamma & -(\mu+\upsilon+\theta)-\lambda & 0 & 0 & 0 \\ 0 & \sigma & \theta & -(\mu+r_1)-\lambda & 0 & 0 \\ 0 & \eta & \upsilon & 0 & -(\delta+\mu+r_2)-\lambda & 0 \\ 0 & 0 & 0 & r_1 & r_2 & -\mu-\lambda \end{vmatrix}.$$

Therefore, FV^{-1} is the next generation matrix of the model structure (3.3). So, as described in [23], $\mathscr{R}_0 = \rho(FV^{-1})$ where ρ stands for spectral radius of the next-generation matrix FV^{-1}. Thus,

$$FV^{-1} = \begin{pmatrix} \frac{\beta\Lambda}{A(\tau+\mu)} & 0 & 0 & 0 \\ 0 & 0 & 0 & 0 \\ 0 & 0 & 0 & 0 \\ 0 & 0 & 0 & 0 \end{pmatrix}.$$

So, $\rho(FV^{-1}) = \frac{\beta\Lambda}{A(\tau+\mu)} = \mathscr{R}_0$, where $A = \gamma+\mu+\eta+\sigma$.

Therefore,

$$\mathscr{R}_0 = \frac{\beta\Lambda}{(\gamma+\mu+\eta+\sigma)(\tau+\mu)} > 0. \tag{3.4}$$

3.3. Local stability analysis of the disease free equilibrium

Theorem 3.1. *The disease free equilibrium DFE is locally asymptotically stable if* $\mathscr{R}_0 < 1$.

Proof. The Jacobian matrix with respect to the system (2.1) is given by:

Simplifying and solving for λ, gives

$$\begin{aligned} \lambda_1 &= -(\tau+\mu) < 0, \\ \lambda_2 &= -(\mu+\upsilon+\theta) < 0, \\ \lambda_3 &= -(\mu+r_1) < 0, \\ \lambda_4 &= -(\delta+\mu+r_2), \\ \lambda_5 &= -\mu < 0, \\ \lambda_6 &= (\gamma+\mu+\eta+\sigma)(\mathscr{R}_0-1) < 0, \text{ provided that } \mathscr{R}_0 < 1. \end{aligned} \tag{3.5}$$

This completes the proof. ■

3.4. Existence of endemic equilibrium point

In this subsection, we look at the existence of endemic equilibrium point. Let us denote the endemic equilibrium by $E_1 = (S^*, E^*, Q^*, I_A^*, I_S^*, R^*)$. For simplicity, $S(t) = S, E(t) = E, Q(t) = Q, I_A(t) = I_A, I_S(t) = I_S$ and $R(t) = R$, will be used henceforth. This endemic equilibrium always satisfies:

$$\begin{aligned} 0 &= \Lambda - (\tau+\mu)S^* - \beta S^* E^*, \\ 0 &= \beta S^* E^* - (\gamma+\mu+\eta+\sigma)E^*, \\ 0 &= \tau S^* + \gamma E^* - (\mu+\upsilon+\theta)Q^*, \\ 0 &= \sigma E^* + \theta Q^* - (\mu+r_1)I_A^*, \\ 0 &= \eta E^* + \upsilon Q^* - (\delta+\mu+r_2)I_S^*, \\ 0 &= r_1 I_A^* + r_2 I_S^* - \mu R^*. \end{aligned} \tag{3.6}$$

From the first Equation of (3.6), we obtain

$$S^* = \frac{\Lambda}{\gamma+\mu+\beta E^*}. \tag{3.7}$$

Inserting (3.7) in the second Equation of (3.6), we get

$$E^* = \frac{(\tau+\mu)}{\beta}(\mathscr{R}_0 - 1). \tag{3.8}$$

Substituting E^* in (3.7), yields

$$S^* = \frac{\gamma+\mu+\eta+\sigma}{\beta}. \tag{3.9}$$

Using (3.8) and (3.9) in the third Equation of (3.6), gives

$$Q^* = \frac{\tau\beta(\gamma+\mu+\eta+\sigma)+\gamma(\tau+\mu)}{\beta(\mu+\upsilon+\theta)}(\mathscr{R}_0 - 1). \tag{3.10}$$

Substituting Eqs. (3.8) and (3.10), in the fourth Equation of (3.6), we have

$$I_A^* = \frac{(\tau+\mu)[\sigma(\mu+\upsilon+\theta)+\gamma\theta]}{\beta(\mu+\upsilon+\theta)(\mu+r_1)}(\mathscr{R}_0 - 1). \tag{3.11}$$

Inserting Eqs. (3.8) and (3.10), in the fifth equation of (3.6) we get

$$I_S^* = \frac{(\tau+\mu)[\eta(\mu+\upsilon+\theta)+\tau\beta\upsilon(\gamma+\upsilon+\eta+\sigma)+\gamma]}{\beta(\mu+\upsilon+\theta)(\delta+\mu+r_2)}(\mathscr{R}_0 - 1). \tag{3.12}$$

Bringing Eqs. (3.11) and (3.12), into the sixth equation of (3.6), yields

$$\begin{aligned} R^* &= \frac{1}{\mu}\left[\frac{[(\tau+\mu)[\sigma(\mu+\upsilon+\theta)+\gamma\theta]]r_1}{\beta(\mu+\upsilon+\theta)(\mu+r_1)}\right. \\ &\left. + \frac{[(\tau+\mu)[\eta(\mu+\upsilon+\theta)+\tau\beta\upsilon(\gamma+\upsilon+\eta+\sigma)+\gamma]]r_2}{\beta(\mu+\upsilon+\theta)(\delta+\mu+r_2)}\right](\mathscr{R}_0 - 1). \end{aligned} \tag{3.13}$$

Thus, we conclude with the following theorem.

Theorem 3.2. *The system (2.1) has unique endemic equilibrium point given by*

$$E_1 = \left(\frac{\gamma+\mu+\eta+\sigma}{\beta}, a(\mathscr{R}_0-1), b(\mathscr{R}_0-1), c(\mathscr{R}_0-1), d(\mathscr{R}_0-1), \frac{(cr_1+dr_2)}{\mu}(\mathscr{R}_0-1)\right),$$

whenever $\mathscr{R}_0 > 1$ *and*

$$\begin{aligned} a &= \frac{(\tau+\mu)}{\beta}, \\ b &= \frac{\tau\beta(\gamma+\mu+\eta+\sigma)+\gamma(\tau+\mu)}{\beta(\mu+\upsilon+\theta)}, \\ c &= \frac{(\tau+\mu)[\sigma(\mu+\upsilon+\theta)+\gamma\theta]}{\beta(\mu+\upsilon+\theta)(\mu+r_1)}, \\ d &= \frac{(\tau+\mu)[\eta(\mu+\upsilon+\theta)+\tau\beta\upsilon(\gamma+\upsilon+\eta+\sigma)+\gamma]}{\beta(\mu+\upsilon+\theta)(\delta+\mu+r_2)}. \end{aligned}$$

3.5. Local stability analysis of the endemic equilibrium E_1

Theorem 3.3. *The endemic equilibrium E_1 is locally asymptotically stable if $\mathscr{R}_0 > 1$.*

Proof. The Jacobian matrix with respect to the system (2.1) is given by:

$$J = \begin{pmatrix} -(\tau+\mu)-\beta E & -\beta S & 0 & 0 & 0 & 0 \\ \beta E & \beta S-(\gamma+\mu+\eta+\sigma) & 0 & 0 & 0 & 0 \\ \tau & \gamma & -(\mu+\upsilon+\theta) & 0 & 0 & 0 \\ 0 & \sigma & \theta & -(\mu+r_1) & 0 & 0 \\ 0 & \eta & \upsilon & 0 & -(\delta+\mu+r_2) & 0 \\ 0 & 0 & 0 & r_1 & r_2 & -\mu \end{pmatrix},$$

which implies,

$$J_{E_1} = \begin{pmatrix} -(\tau+\mu)\mathscr{R}_0 & -(\gamma+\mu+\eta+\sigma) & 0 & 0 & 0 & 0 \\ \gamma+\mu+\eta+\sigma & 0 & 0 & 0 & 0 & 0 \\ \tau & \gamma & -(\mu+\upsilon+\theta) & 0 & 0 & 0 \\ 0 & \sigma & \theta & -(\mu+r_1) & 0 & 0 \\ 0 & \eta & \upsilon & 0 & -(\delta+\mu+r_2) & 0 \\ 0 & 0 & 0 & r_1 & r_2 & -\mu \end{pmatrix}.$$

The characteristic polynomial of the Jacobian matrix at E_1 is given by $det(J_{E_1} - \lambda I) = 0$. where λ is the eigenvalue and I is 6×6 identity matrix. Thus,

$$det(J_{E_1} - \lambda I) = \begin{vmatrix} (\tau+\mu)\mathscr{R}_0 - \lambda & -(\gamma+\mu+\eta+\sigma) & 0 & 0 & 0 & 0 \\ \gamma+\mu+\eta+\sigma & -\lambda & 0 & 0 & 0 & 0 \\ \tau & \gamma & -(\mu+\upsilon+\theta)-\lambda & 0 & 0 & 0 \\ 0 & \sigma & \theta & -(\mu+r_1)-\lambda & 0 & 0 \\ 0 & \eta & \upsilon & 0 & -(\delta+\mu+r_2)-\lambda & 0 \\ 0 & 0 & 0 & r_1 & r_2 & -\mu-\lambda \end{vmatrix}.$$

$$= [\lambda^2 + (\tau+\mu)\mathscr{R}_0\lambda + (\gamma+\mu+\eta+\sigma)^2][-(\mu+\upsilon+\theta)-\lambda][-(\mu+r_1)-\lambda][-(\delta+\mu+r_2)-\lambda](-\mu-\lambda)$$

Simplifying the characteristic polynomial (i.e making the characteristic equation) and solving for λ, gives

$$\begin{aligned} \lambda_1 &= -(\mu+\upsilon+\theta) < 0, \\ \lambda_2 &= -(\mu+r_1) < 0, \\ \lambda_3 &= -(\delta+\mu+r_2) < 0, \\ \lambda_4 &= -\mu < 0. \end{aligned} \tag{3.14}$$

The quadratic $\lambda^2 + (\tau+\mu)\mathscr{R}_0\lambda + (\gamma+\mu+\eta+\sigma)^2$ has all terms positive and thus, its roots must all be negative. Meanings $\lambda_{5,6} < 0$. This com-

pletes the proof. ■

3.6. Global stability analysis of the endemic equilibrium E_1

Theorem 3.4. *The system (2.1) has no periodic orbits.*

Proof. We employ the Dulac's criterion to achieve this. Now, let $X = (S, E, Q, I_A, I_S, R)$. Taking the Dulac's function

$$G = \frac{1}{SE},$$

we obtain

$$\begin{aligned}
G\frac{dS}{dt} &= \frac{\Lambda}{SE} - \frac{(\tau+\mu)}{E} - \beta,\\
G\frac{dE}{dt} &= \beta - \frac{(\gamma+\mu+\eta+\sigma)}{S},\\
G\frac{dQ}{dt} &= \frac{\tau}{E} + \frac{\gamma}{S} - \frac{(\mu+\upsilon+\theta)Q}{SE},\\
G\frac{dI_A}{dt} &= \frac{\sigma}{S} + \frac{\theta Q}{SE} - \frac{(\mu+r_1)I_A}{SE},\\
G\frac{dI_S}{dt} &= \frac{\eta}{S} + \frac{\upsilon Q}{SE} - \frac{(\delta+\mu+r_2)I_S}{SE},\\
G\frac{dR}{dt} &= \frac{r_1 I_A}{SE} + \frac{r_2 I_S}{SE} - \frac{\mu R}{SE}.
\end{aligned} \tag{3.15}$$

Thus,

$$\begin{aligned}
\frac{dGX}{dt} &= \frac{\partial}{\partial S}\left(G\frac{dS}{dt}\right) + \frac{\partial}{\partial E}\left(G\frac{dE}{dt}\right) + \frac{\partial}{\partial Q}\left(G\frac{dQ}{dt}\right) + \frac{\partial}{\partial I_A}\left(G\frac{dI_A}{dt}\right)\\
&+\frac{\partial}{\partial I_S}\left(G\frac{dI_S}{dt}\right) + \frac{\partial}{\partial R}\left(G\frac{dR}{dt}\right)\\
&= \frac{\partial}{\partial S}\left(\frac{\Lambda}{SE} - \frac{(\tau+\mu)}{E} - \beta\right) + \frac{\partial}{\partial E}\left(\beta - \frac{(\gamma+\mu+\eta+\sigma)}{S}\right)\\
&+\frac{\partial}{\partial Q}\left(\frac{\tau}{E} + \frac{\gamma}{S} - \frac{(\mu+\upsilon+\theta)Q}{SE}\right)\\
&+\frac{\partial}{\partial I_A}\left(\frac{\sigma}{S} + \frac{\theta Q}{SE} - \frac{(\mu+r_1)I_A}{SE}\right) + \frac{\partial}{\partial I_S}\left(\frac{\eta}{S} + \frac{\upsilon Q}{SE} - \frac{(\delta+\mu+r_2)I_S}{SE}\right)\\
&+\frac{\partial}{\partial R}\left(\frac{r_1 I_A}{SE} + \frac{r_2 I_S}{SE} - \frac{\mu R}{SE}\right),\\
&= -\frac{\Lambda}{S^2 E} - \frac{(\mu+\upsilon+\theta)}{SE} - \frac{(\mu+r_1)}{SE} - \frac{(\delta+\mu+r_2)}{SE} - \frac{\mu}{SE},\\
&= -\left(\frac{\Lambda}{S^2 E} + \frac{\delta+4\mu+\upsilon+r_1+r_2+\theta}{SE}\right),\\
&< 0.
\end{aligned}$$

Hence, the system (2.1) has no periodic orbit. This completes the proof. ■ Since Ω is positively invariant, it follows from Poincarè-Bendixson theorem that all solutions of the system (2.1) originate and remain in Ω for all t. We conclude with the following theorem:

Theorem 3.5. *The endemic equilibrium E_1 for the system (2.1) is globally asymptotically stable whenever $\mathscr{R}_0 > 1$.*

4. Fractional order model in the sense of ABC-fractional operator

In the current research work, researchers have shown that mathematical models constructed with the aid of fractional operators are often more precise and reliable compared to the integer-order case due to the enhanced degree of freedom. In fractional-order models, the memory property allows more knowledge from the past to be added, which predicts and translates models more accurately. Recently, Atangana and Baleanu [16], introduced new fractional derivatives without singularity and locality. The non-singularity and non-locality of the kernel give a better description of the memory. The aforementioned operator has found wide applications to model dynamics processes in many well-known fields of science, engineering, biology, medicine, and many other, see [31,45,5,17,] and the references cited therein. Besides, in comparisons with classical Caputo, Caputo-Fabrizio, the ABC operator recorded the highest efficiency in terms of experimental data and numerical efficiency [42].

Motivated by the above-mentioned application, in this section, we generalize the proposed model (2.1) to fractional order in the sense of ABC-fractional derivative and study the existence and uniqueness of solutions for the generalized model using the techniques of fixed point theorems. Now, before we generalize the model (2.1), we recall some preliminaries definitions which are important throughout the section.

Definition 4.1. ([16]) For a given function $z \in \mathscr{H}^1(0,T), T > 0$ and $\alpha > 0$. The fractional operator

$${}^{ABC}D^{\alpha}_{0^+} z(t) = \frac{N(\alpha)}{1-\alpha}\int_0^t E_\alpha\left[\frac{-\alpha}{1-\alpha}(t-x)^\alpha\right] z'(x)dx, \tag{4.1}$$

is called the ABC-fractional operator where $N(r)$ represent the normalization function and satisfies $N(0) = N(1) = 1$ and $E_\alpha(\cdot)$ denotes the one-parameter Mittag–Leffler function of form:

$$E_\alpha(u) = \sum_{k=0}^{\infty} \frac{u^k}{\Gamma(\alpha k + 1)}. \tag{4.2}$$

Definition 4.2. ([16]) The fractional operator

$${}^{AB}I^{\alpha}_{0^+} z(t) = \frac{1-\alpha}{N(\alpha)} z(t) + \frac{\alpha}{N(\alpha)\Gamma(\alpha)}\int_0^t (t-x)^{\alpha-1} z(x)dx, t > 0, \tag{4.3}$$

is referred to fractional integral operator associated with ABC-fractional derivative. Therefore, the proposed nonlinear fractional model in the sense of ABC-fractional operator is of the form:

$$\begin{aligned}
{}^{ABC}D^{\alpha}_0 S(t) &= \Lambda^\alpha - (\tau^\alpha + \mu^\alpha)S(t) - \beta^\alpha S(t)E(t),\\
{}^{ABC}D^{\alpha}_0 E(t) &= \beta^\alpha S(t)E(t) - (\gamma^\alpha + \mu^\alpha + \eta^\alpha + \sigma^\alpha)E(t),\\
{}^{ABC}D^{\alpha}_0 Q(t) &= \tau^\alpha S(t) + \gamma^\alpha E(t) - (\mu^\alpha + \upsilon^\alpha + \theta^\alpha)Q(t),\\
{}^{ABC}D^{\alpha}_0 I_A(t) &= \sigma^\alpha E(t) + \theta^\alpha Q(t) - (\mu^\alpha + r_1^\alpha)I_A(t),\\
{}^{ABC}D^{\alpha}_0 I_S(t) &= \eta^\alpha E(t) + \upsilon^\alpha Q(t) - (\delta^\alpha + \mu^\alpha + r_2^\alpha)I_S(t),\\
{}^{ABC}D^{\alpha}_0 R(t) &= r_1^\alpha I_A(t) + r_2^\alpha I_S(t) - \mu^\alpha R(t),
\end{aligned} \tag{4.4}$$

where ${}^{ABC}D^{\alpha}_0(\cdot)$ is the ABC-fractional derivative of order $(0 < \alpha \le 1)$ and the variables are assumed to be non-negative with appropriate initial conditions.

Remark 1. It is worth mentioning here that, the parameters are assumed to be non-negative and have dimension time. In this paper, the dimensionality consistency was taking into consideration when fictionalized the integer-order model as the dimension of each left-hand side equation carries $time^{-\alpha}$, $(\alpha > 0)$, whereas the right sides remains dimensionally $time^{-1}$. This technique was proposed by Diethelm in [24].

4.1. Existence and uniqueness result

This subsection presents the existence and uniqueness of solutions of the proposed model using the techniques of fixed point theory. Here, we denote $\mathbf{E} = \mathscr{C}([0,T], \mathbb{R})$ the Banach space of all continuous real-valued function equipped with the norm defined by

$$\|(S, E, Q, I_A, I_S, R)\| = \|S(t)\| + \|E(t)\| + \|Q(t)\| + \|I_A(t)\| + \|I_S(t)\| + \|R(t)\|,$$

where

$$\|S\| = \sup_{t\in[0,T]} |S(t)|, \quad \|E\| = \sup_{t\in[0,T]} |E(t)|, \quad \|Q\| = \sup_{t\in[0,T]} |Q(t)|,$$

$$\|I_A\| = \sup_{t\in[0,T]}|I_A(t)|, \quad \|I_S\| = \sup_{t\in[0,T]}|I_S(t)| \text{ and } \|R\| = \sup_{t\in[0,T]}|R(t)|.$$

Now, applying the fractional integral operator ${}^{AB}I^{\alpha}_{0^+}$ on both sides of system (4.4), yields

$$\begin{aligned}
S(t)-S(0) &= {}^{AB}I^{\alpha}_{0^+}\{\Lambda^{\alpha}-(\tau^{\alpha}+\mu^{\alpha})S(t)-\beta^{\alpha}S(t)E(t)\},\\
E(t)-E(0) &= {}^{AB}I^{\alpha}_{0^+}\{\beta^{\alpha}S(t)E(t)-(\gamma^{\alpha}+\mu^{\alpha}+\eta^{\alpha}+\sigma^{\alpha})E(t)\},\\
Q(t)-Q(0) &= {}^{AB}I^{\alpha}_{0^+}\{\tau^{\alpha}S(t)+\gamma^{\alpha}E(t)-(\mu^{\alpha}+\upsilon^{\alpha}+\theta^{\alpha})Q(t)\},\\
I_A(t)-I_A(0) &= {}^{AB}I^{\alpha}_{0^+}\{\sigma^{\alpha}E(t)+\theta^{\alpha}Q(t)-(\mu^{\alpha}+r_1^{\alpha})I_A(t)\},\\
I_S(t)-I_S(0) &= {}^{AB}I^{\alpha}_{0^+}\{\eta^{\alpha}E(t)+\upsilon^{\alpha}Q(t)-(\delta^{\alpha}+\mu^{\alpha}+r_2^{\alpha})I_S(t)\},\\
R(t)-R(0) &= {}^{AB}I^{\alpha}_{0^+}\{r_1^{\alpha}I_A(t)+r_2^{\alpha}I_S(t)-\mu^{\alpha}R(t)\},
\end{aligned} \tag{4.5}$$

which implies

$$\begin{aligned}
S(t) &= S(0)+\frac{1-\alpha}{N(\alpha)}F_1(t,S(t))+\frac{\alpha}{N(\alpha)}\frac{1}{\Gamma(\alpha)}\int_0^t(t-x)^{\alpha-1}F_1(x,S(x))dx,\\
E(t) &= E(0)+\frac{1-\alpha}{N(\alpha)}F_2(t,E(t))+\frac{\alpha}{N(\alpha)}\frac{1}{\Gamma(\alpha)}\int_0^t(t-x)^{\alpha-1}F_2(x,E(x))dx,\\
Q(t) &= Q(0)+\frac{1-\alpha}{N(\alpha)}F_3(t,Q(t))+\frac{\alpha}{N(\alpha)}\frac{1}{\Gamma(\alpha)}\int_0^t(t-x)^{\alpha-1}F_3(x,Q(x))dx,\\
I_A(t) &= I_A(0)+\frac{1-\alpha}{N(\alpha)}F_4(t,I_A(t))+\frac{\alpha}{N(\alpha)}\frac{1}{\Gamma(\alpha)}\int_0^t(t-x)^{\alpha-1}F_4(x,I_A(x))dx,\\
I_S(t) &= I_S(0)+\frac{1-\alpha}{N(\alpha)}F_5(t,I_S(t))+\frac{\alpha}{N(\alpha)}\frac{1}{\Gamma(\alpha)}\int_0^t(t-x)^{\alpha-1}F_5(x,I_S(x))dx,\\
R(t) &= R(0)+\frac{1-\alpha}{N(\alpha)}F_6(t,R(t))+\frac{\alpha}{N(\alpha)}\frac{1}{\Gamma(\alpha)}\int_0^t(t-x)^{\alpha-1}F_6(x,R(x))dx,
\end{aligned} \tag{4.6}$$

where

$$\begin{aligned}
F_1(t,S(t)) &= \Lambda^{\alpha}-(\tau^{\alpha}+\mu^{\alpha})S(t)-\beta^{\alpha}S(t)E(t),\\
F_2(t,E(t)) &= \beta^{\alpha}S(t)E(t)-(\gamma^{\alpha}+\mu^{\alpha}+\eta^{\alpha}+\sigma^{\alpha})E(t),\\
F_3(t,Q(t)) &= \tau^{\alpha}S(t)+\gamma^{\alpha}E(t)-(\mu^{\alpha}+\upsilon^{\alpha}+\theta^{\alpha})Q(t),\\
F_4(t,I_A(t)) &= \sigma^{\alpha}E(t)+\theta^{\alpha}Q(t)-(\mu^{\alpha}+r_1^{\alpha})I_A(t),\\
F_5(t,I_S(t)) &= \eta^{\alpha}E(t)+\upsilon^{\alpha}Q(t)-(\delta^{\alpha}+\mu^{\alpha}+r_2^{\alpha})I_S(t),\\
F_6(t,R(t)) &= r_1^{\alpha}I_A(t)+r_2^{\alpha}I_S(t)-{}^{!}\,''substring-after(preceding-sibling::comment()[starts-with(.,'hskip')][1],'hskip')''pt>\mu^{\alpha}R(t).
\end{aligned} \tag{4.7}$$

The kernels in Equations (4.7) satisfies the Lipschitz condition for $0\leqslant M_i<1$, $i=1,2,\ldots6$, if and only if the nonlinear functions $S(t), E(t), Q(t), I_A(t), I_S(t)$ and $R(t)$ have an upper bound. Indeed, suppose $S(t)$ and $S^*(t)$ be two functions, then we get

$$\begin{aligned}
\|F_1(t,S(t))-F_1(t,S^*(t))\| &= \|\Lambda^{\alpha}-(\tau^{\alpha}+\mu^{\alpha})S(t)-\beta^{\alpha}S(t)E(t)\\
&\quad -(\Lambda^{\alpha}-(\tau^{\alpha}+\mu^{\alpha})S^*(t)-\beta^{\alpha}S^*(t)E(t))\|\\
&= \|(\tau^{\alpha}+\mu^{\alpha})(S^*(t)-S(t))+\beta^{\alpha}E(t)(S^*(t)-S(t))\|\\
&\leqslant \left((\tau^{\alpha}+\mu^{\alpha})+\beta^{\alpha}\sup_{t\in[0,T]}|E(t)|\right)\|S(t)-S^*(t)\|\\
&= M_1\|S(t)-S^*(t)\|,
\end{aligned} \tag{4.8}$$

where $M_1 = \left(\left(\tau^{\alpha}+\mu^{\alpha}\right)+\beta^{\alpha}\sup_{t\in[0,T]}|E(t)|\right)$. Thus,

$$\|F_1(t,S(t))-F_1(t,S^*(t))\|\leqslant M_1\|S(t)-S^*(t)\|. \tag{4.9}$$

Repeating the same procedure as in Eq. (4.8) above, we have

$$\begin{aligned}
\|F_2(t,E(t))-F_2(t,E^*(t))\| &\leqslant M_2\|E(t)-E^*(t)\|,\\
\|F_3(t,Q(t))-F_3(t,Q^*(t))\| &\leqslant M_3\|Q(t)-Q^*(t)\|,\\
\|F_4(t,I_A(t))-F_4(t,I_A^*(t))\| &\leqslant M_4\|I_A(t)-I_A^*(t)\|,\\
\|F_5(t,I_S(t))-F_5(t,I_S^*(t))\| &\leqslant M_5\|I_S(t)-I_S^*(t)\|,\\
\|F_6(t,R(t))-F_6(t,R^*(t))\| &\leqslant M_6\|R(t)-R^*(t)\|,
\end{aligned} \tag{4.10}$$

where M_i $(i=1,2,\ldots6)$ are the corresponding Lipschitz constant for the functions $F_i(\cdot)$ for $i=1,2,\ldots,6$.

Now, Eq. (4.6) can be written in recursive form given by

$$\begin{aligned}
S_n(t) &= S(0)+\frac{1-\alpha}{N(\alpha)}F_1(t,S_{n-1}(t))\\
&\quad +\frac{\alpha}{N(\alpha)}\frac{1}{\Gamma(\alpha)}\int_0^t(t-x)^{\alpha-1}F_1(x,S_{n-1}(x))dx,\\
E_n(t) &= E(0)+\frac{1-\alpha}{N(\alpha)}F_2(t,E_{n-1}(t))\\
&\quad +\frac{\alpha}{N(\alpha)}\frac{1}{\Gamma(\alpha)}\int_0^t(t-x)^{\alpha-1}F_2(x,E_{n-1}(x))dx,\\
Q_n(t) &= Q(0)+\frac{1-\alpha}{N(\alpha)}F_3(t,Q_{n-1}(t))\\
&\quad +\frac{\alpha}{N(\alpha)}\frac{1}{\Gamma(\alpha)}\int_0^t(t-x)^{\alpha-1}F_3(x,Q_{n-1}(x))dx,\\
I_{A,n}(t) &= I_A(0)+\frac{1-\alpha}{N(\alpha)}F_4(t,I_{A,n-1}(t))\\
&\quad +\frac{\alpha}{N(\alpha)}\frac{1}{\Gamma(\alpha)}\int_0^t(t-x)^{\alpha-1}F_4(x,I_{A,n-1}(x))dx,\\
I_{S,n}(t) &= I_A(0)+\frac{1-\alpha}{N(\alpha)}F_5(t,I_{S,n-1}(t))\\
&\quad +\frac{\alpha}{N(\alpha)}\frac{1}{\Gamma(\alpha)}\int_0^t(t-x)^{\alpha-1}F_5(x,I_{S,n-1}(x))dx,\\
R_n(t) &= R(0)+\frac{1-\alpha}{N(\alpha)}F_6(t,R_{n-1}(t))\\
&\quad +\frac{\alpha}{N(\alpha)}\frac{1}{\Gamma(\alpha)}\int_0^t(t-x)^{\alpha-1}F_6(x,R_{n-1}(x))dx.
\end{aligned} \tag{4.11}$$

Let us denote difference between successive components by Φ_n^i, $i=1,2,\ldots6$. So,

$$
\begin{aligned}
\Phi_n^1(t) &= S_n(t) - S_{n-1}(t) = \frac{1-\alpha}{N(\alpha)}(F_1(t, S_{n-1}(t)) - F_1(t, S_{n-2}(t))) \\
&+\frac{\alpha}{N(\alpha)}\frac{1}{\Gamma(\alpha)}\int_0^t (t-x)^{\alpha-1}(F_1(x, S_{n-1}(x)) - F_1(x, S_{n-2}(x)))dx, \\
\Phi_n^2(t) &= E_n(t) - E_{n-1}(t) = \frac{1-\alpha}{N(\alpha)}(F_2(t, E_{n-1}(t)) - F_2(t, E_{n-2}(t))) \\
&+\frac{\alpha}{N(\alpha)}\frac{1}{\Gamma(\alpha)}\int_0^t (t-x)^{\alpha-1}(F_2(x, E_{n-1}(x)) - F_2(x, E_{n-2}(x)))dx, \\
\Phi_n^3(t) &= Q_n(t) - Q_{n-1}(t) = \frac{1-\alpha}{N(\alpha)}(F_3(t, Q_{n-1}(t)) - F_3(t, Q_{n-2}(t))) \\
&+\frac{\alpha}{N(\alpha)}\frac{1}{\Gamma(\alpha)}\int_0^t (t-x)^{\alpha-1}(F_3(x, Q_{n-1}(x)) - F_3(x, Q_{n-2}(x)))dx, \\
\Phi_n^4(t) &= I_{A,n}(t) - I_{A,n-1}(t) = \frac{1-\alpha}{N(\alpha)}(F_4(t, I_{A,n-1}(t)) - F_4(t, I_{A,n-2}(t))) \\
&+\frac{\alpha}{N(\alpha)}\frac{1}{\Gamma(\alpha)}\int_0^t (t-x)^{\alpha-1}(F_4(x, I_{A,n-1}(x)) - F_4(x, I_{A,n-2}(x)))dx, \\
\Phi_n^5(t) &= I_{S,n}(t) - I_{S,n-1}(t) = \frac{1-\alpha}{N(\alpha)}(F_5(t, I_{S,n-1}(t)) - F_5(t, I_{S,n-2}(t))) \\
&+\frac{\alpha}{N(\alpha)}\frac{1}{\Gamma(\alpha)}\int_0^t (t-x)^{\alpha-1}(F_5(x, I_{S,n-1}(x)) - F_5(x, I_{S,n-2}(x)))dx, \\
\Phi_n^6(t) &= R_n(t) - R_{n-1}(t) = \frac{1-\alpha}{N(\alpha)}(F_6(t, R_{n-1}(t)) - F_6(t, R_{n-2}(t))) \\
&+\frac{\alpha}{N(\alpha)}\frac{1}{\Gamma(\alpha)}\int_0^t (t-x)^{\alpha-1}(F_6(x, R_{n-1}(x)) - F_6(x, R_{n-2}(x)))dx,
\end{aligned} \tag{4.12}
$$

taking into consideration that $S_n(t) = \sum_{i=0}^n \Phi_i^1(t)$, $E_n(t) = \sum_{i=0}^n \Phi_i^1(t)$, $Q_n(t) = \sum_{i=0}^n \Phi_i^1(t)$, $I_{A,n}(t) = \sum_{i=0}^n \Phi_i^1(t)$, $I_{S,n}(t) = \sum_{i=0}^n \Phi_i^1(t)$, $R_n(t) = \sum_{i=0}^n \Phi_i^1(t)$. Taking the norm on both side of Equations (4.12) and using Equations (4.9) yields

$$
\begin{aligned}
\|\Phi_n^1(t)\| &= \frac{1-\alpha}{N(\alpha)}M_1\|\Phi_{n-1}^1(t)\| + \frac{\alpha}{N(\alpha)}\frac{M_1}{\Gamma(\alpha)}\int_0^t (t-x)^{\alpha-1}\|\Phi_{n-1}^1(x)\|dx, \\
\|\Phi_n^2(t)\| &= \frac{1-\alpha}{N(\alpha)}M_2\|\Phi_{n-1}^2(t)\| + \frac{\alpha}{N(\alpha)}\frac{M_2}{\Gamma(\alpha)}\int_0^t (t-x)^{\alpha-1}\|\Phi_{n-1}^2(x)\|dx, \\
\|\Phi_n^3(t)\| &= \frac{1-\alpha}{N(\alpha)}M_3\|\Phi_{n-1}^3(t)\| + \frac{\alpha}{N(\alpha)}\frac{M_3}{\Gamma(\alpha)}\int_0^t (t-x)^{\alpha-1}\|\Phi_{n-1}^3(x)\|dx, \\
\|\Phi_n^4(t)\| &= \frac{1-\alpha}{N(\alpha)}M_4\|\Phi_{n-1}^4(t)\| + \frac{\alpha}{N(\alpha)}\frac{M_4}{\Gamma(\alpha)}\int_0^t (t-x)^{\alpha-1}\|\Phi_{n-1}^4(x)\|dx, \\
\|\Phi_n^5(t)\| &= \frac{1-\alpha}{N(\alpha)}M_5\|\Phi_{n-1}^5(t)\| + \frac{\alpha}{N(\alpha)}\frac{M_5}{\Gamma(\alpha)}\int_0^t (t-x)^{\alpha-1}\|\Phi_{n-1}^5(x)\|dx, \\
\|\Phi_n^6(t)\| &= \frac{1-\alpha}{N(\alpha)}M_6\|\Phi_{n-1}^6(t)\| + \frac{\alpha}{N(\alpha)}\frac{M_6}{\Gamma(\alpha)}\int_0^t (t-x)^{\alpha-1}\|\Phi_{n-1}^6(x)\|dx.
\end{aligned} \tag{4.13}
$$

Now, we are ready to state and prove the main theorem based on the above results.

Theorem 4.3. *The fractional proposed model (4.4) possesses a unique solution for $t \in [0, T]$ if the condition is satisfied*

$$
\left(\frac{1-\alpha}{N(\alpha)}M_i + \frac{1}{N(\alpha)}\frac{M_i}{\Gamma(r)}T^\alpha\right) \langle 1, \ i = 1, 2, \ldots, 6. \tag{4.14}
$$

Proof. Since from the assumptions the functions $S(t), E(t), Q(t), I_A(t), I_S(t), R(t)$ are bounded and satisfies the Lipschitz condition. Thus, in view of Eq. (4.13), we get

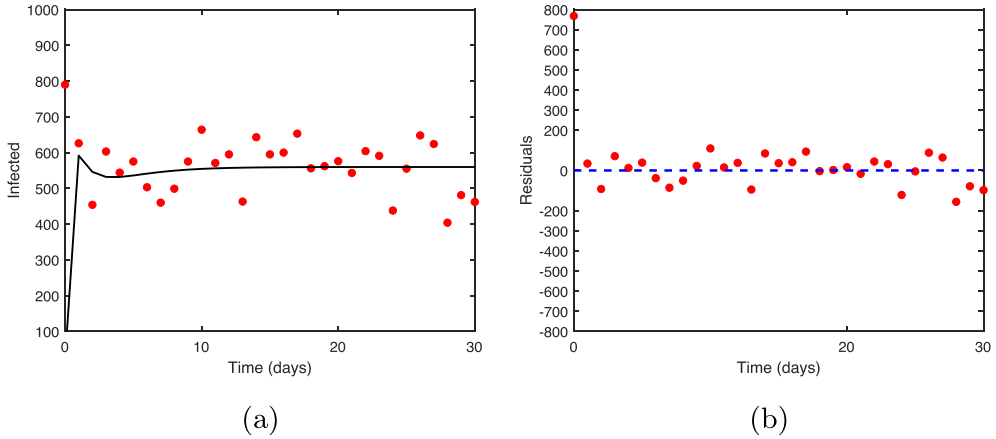

Fig. 5.3. The daily COVID-19 cumulative cases time series in Nigeria from 1 July to July 31, 2020, with the best-fitted curve from simulations of the proposed model and (b) the residuals for the best-fitted curve.

Table 2
Baseline values of the parameters used in the model (2.1).

Fitted parameter	Value (Range)	Units/remarks	Sources
τ	0.0002	day^{-1}	Fitted
β	0.0805	day^{-1}	Fitted
δ	$1.6728e-5$	day^{-1}	Fitted
γ	$2.0138e-4$	day^{-1}	Fitted
η	0.4478	day^{-1}	Assumed
θ	0.0101	day^{-1}	Assumed
μ	0.0106	day^{-1}	Fitted
υ	$3.2084e-4$	day^{-1}	Fitted
σ	0.0668	day^{-1}	Assumed
Λ	0.02537	day^{-1}	Assumed
r_1	$5.7341e-5$	day^{-1}	Assumed
r_2	$1.6728e-5$	day^{-1}	Assumed

$$
\begin{aligned}
\|\Phi_n^1(t)\| &\leqslant \|S_n(0)\|\left(\frac{1-\alpha}{N(\alpha)}M_1+\frac{1}{N(\alpha)}\frac{M_1}{\Gamma(\alpha)}T^\alpha\right)^n,\\
\|\Phi_n^2(t)\| &\leqslant \|E_n(0)\|\left(\frac{1-\alpha}{N(\alpha)}M_2+\frac{1}{N(\alpha)}\frac{M_2}{\Gamma(\alpha)}T^\alpha\right)^n,\\
\|\Phi_n^3(t)\| &\leqslant \|Q_n(0)\|\left(\frac{1-\alpha}{N(\alpha)}M_3+\frac{1}{N(\alpha)}\frac{M_3}{\Gamma(\alpha)}T^\alpha\right)^n,\\
\|\Phi_n^4(t)\| &\leqslant \|I_{A,n}(0)\|\left(\frac{1-\alpha}{N(\alpha)}M_4+\frac{1}{N(\alpha)}\frac{M_4}{\Gamma(\alpha)}T^\alpha\right)^n,\\
\|\Phi_n^5(t)\| &\leqslant \|I_{S,n}(0)\|\left(\frac{1-\alpha}{N(\alpha)}M_5+\frac{1}{N(\alpha)}\frac{M_5}{\Gamma(\alpha)}T^\alpha\right)^n,\\
\|\Phi_n^6(t)\| &\leqslant \|R_n(0)\|\left(\frac{1-\alpha}{N(\alpha)}M_6+\frac{1}{N(\alpha)}\frac{M_6}{\Gamma(\alpha)}T^\alpha\right)^n.
\end{aligned}
\tag{4.15}
$$

Hence, the sequences above exist and as $n\longrightarrow\infty, \|\Phi_n^i(t)\|\longrightarrow 0,\ i=1,2,\ldots 6$. Also, utilizing the triangular inequality for any k, Eq. (4.15) yields

$$
\begin{aligned}
\|S_{n+k}(t)-S_n(t)\| &\leqslant \sum_{i=n+1}^{n+k} P_1^i = \frac{P_1^{n+1}-P_1^{n+k+1}}{1-P_1},\\
\|E_{n+k}(t)-E_n(t)\| &\leqslant \sum_{i=n+1}^{n+k} P_2^i = \frac{P_2^{n+1}-P_2^{n+k+1}}{1-P_2},\\
\|Q_{n+k}(t)-Q_n(t)\| &\leqslant \sum_{i=n+1}^{n+k} P_3^i = \frac{P_3^{n+1}-P_3^{n+k+1}}{1-P_3},\\
\|I_{A,n+k}(t)-I_{A,n}(t)\| &\leqslant \sum_{i=n+1}^{n+k} P_4^i = \frac{P_4^{n+1}-P_4^{n+k+1}}{1-P_4},\\
\|I_{S,n+k}(t)-I_{S,n}(t)\| &\leqslant \sum_{i=n+1}^{n+k} P_5^i = \frac{P_5^{n+1}-P_5^{n+k+1}}{1-P_5},\\
\|R_{n+k}(t)-R_n(t)\| &\leqslant \sum_{i=n+1}^{n+k} P_6^i = \frac{P_6^{n+1}-P_6^{n+k+1}}{1-P_6},
\end{aligned}
\tag{4.16}
$$

where the $P_i,\ i=1,2,\ldots 6$, are the terms within the bracket of Equations (4.15) and the condition $\left(\frac{1-\alpha}{N(\alpha)}M_i+\frac{1}{N(\alpha)}\frac{M_i}{\Gamma(\alpha)}T^\alpha\right)<1$. Thus, by uniform convergent theorem the function $S_n,\ E_n,\ Q_n,\ I_{S,n},\ I_{A,n}$ and R_n constitute a Cauchy sequence in **E**. So, applying the limit theory on the equation (4.11) as $n\to\infty$ shows that the limit of these sequences is the unique solution of the proposed model (4.4). In addition, we conclude the existence of a unique solution of the proposed model (4.4). ■

Table 3
The elasticity indices for $\mathscr{R}_0 = 1.703052076$ to the parameters of the model (2.1).

Parameter	Baseline value	Elasticity index
Λ	0.02537	1
β	0.0805	1
τ	0.0002	$-0.1851851852e-1$
γ	$2.0138e-4$	$-0.3832879160e-3$
η	0.4478	−0.8523007686
σ	0.0668	−0.1271408918
μ	0.0106	−1.001656533

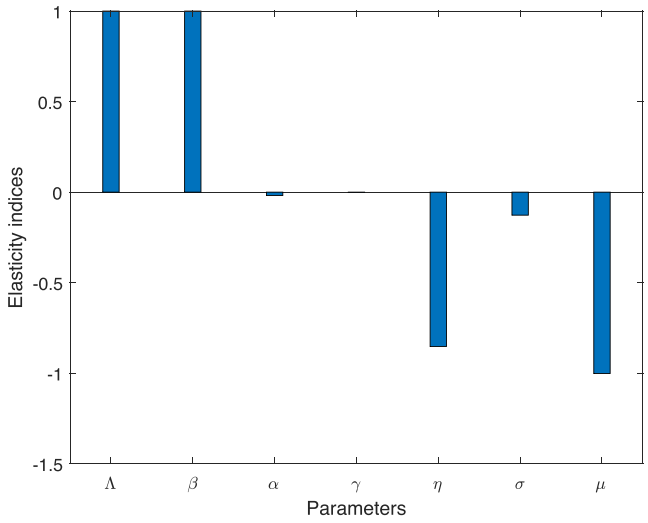

Fig. 5.4. Elasticity indices for significance of parameters in $\mathscr{R}_0$.

5. Model fitting and parameter estimation

One of the essential mechanisms for evaluating the transmission dynamics of a disease is the validation of a newly developed epidemiological model. The availability of real data for the underlying ailment contributes significantly to the completion of this task and the real data gives us an insight into how to determine the best values of some of the model's unknown biological parameters. To this end, we employ the nonlinear least-squares curve fitting method with the help of "*fminsearch*" function from the MATLAB Optimization Toolbox. This approach states that, if a theoretical model $t \mapsto \Xi(t, q_1, q_2, \ldots, q_n)$ is attained and depend on a few unknown parameters $q_1, q_2, \ldots, q_n$ and a sequence of actual data points $(t_0, y_0), \ldots, (t_j, y_j)$ is also at hand then the aim is to obtain values of the parameters so that the error calculated can,

$$
E := \sqrt{\sum_{i=0}^{j} (\Xi(t, q_1, q_2, \ldots, q_n) - y_i)^2}, \tag{5.1}
$$

attain a minimum. 12 biological parameters are associated with the proposed model. Some of these parameters have been assumed while some have been best fitted (see Fig. 5.3). The initial conditions for the state variables are $S(0)=0.5,\ E(0)=0.2,\ Q(0)=0.1,\ I_A(0)=0.2,\ I_S(0)=0.1$ and $R(0)=0$ (see Table 2).

5.1. Sensitivity analysis

In this subsection, the concept of sensitivity analysis is used to discover the robust significance of the generic parameters present in the basic reproduction number $\mathscr{R}_0$. Furthermore, both the analytical and numerical values of the $\mathscr{R}_0$ parameters are derived from precise as-

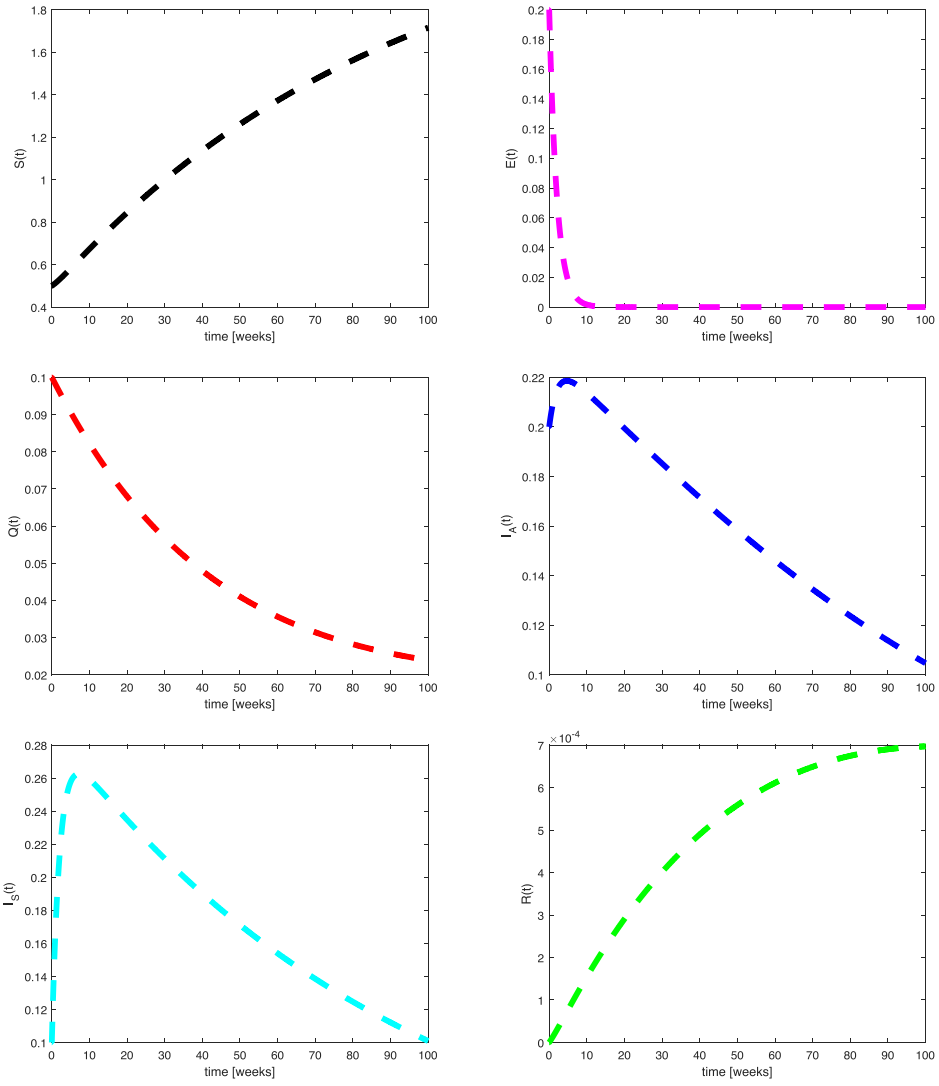

Fig. 5.5. Profiles for behavior of each state variable for the classical version of the model.

sumptions using parameter values. If and only if the dynamics follow the model (2.1), the analytical expressions obtained can be used to shed some light on how to track the model's onset in variant locations. The threshold value $\mathscr{R}_0$ is a quantity known to be the primary way of reducing and aborting the ailment spread by reducing the number to less than unity. The sensitivity index technique is used to measure the most sensitive parameters in the model, those with the positive sign are considered to be highly and proportionally sensitive to the value of $\mathscr{R}_0$ while those with the negative sign are less sensitive to decreasing $\mathscr{R}_0$ and the other category is neutrally sensitive (with zero relative sensitivity). The cause of the transmission of the infringement is commonly recognized to be directly linked to the specific reproduction number $\mathscr{R}_0$. The $\mathscr{R}_0$ elasticity indices is given by Eq. (3.4):

$$\Upsilon_{\mathbf{P_i}}^{\mathscr{R}_0} = \frac{\partial \mathscr{R}_0}{\partial \mathbf{P}_i} \times \frac{\mathbf{P}_i}{\mathscr{R}_0}, \tag{5.2}$$

where $\mathscr{R}_0$ denotes the basic reproduction ratio and $\mathbf{P}_i$ is as stated above. Following the described formula, we reach:

$$\begin{aligned}
\Upsilon_{\Lambda} &= 1,\\
\Upsilon_{\beta} &= 1,\\
\Upsilon_{\tau} &= -\frac{\tau}{\tau+\mu},\\
\Upsilon_{\gamma} &= -\frac{\gamma}{\gamma+\mu+\eta+\sigma},\\
\Upsilon_{\eta} &= -\frac{\eta}{\gamma+\mu+\eta+\sigma},\\
\Upsilon_{\sigma} &= -\frac{\sigma}{\gamma+\mu+\eta+\sigma},\\
\Upsilon_{\mu} &= \mu(\gamma+\mu+\eta+\sigma)(\tau+\mu)\left(-\frac{\Lambda\beta}{(\gamma+\mu+\eta+\sigma)^2(\tau+\mu)}\right.\\
&\quad \left.-\frac{\Lambda\beta}{(\gamma+\mu+\eta+\sigma)(\tau+\mu)^2}\right)\Lambda^{-1}\beta^{-1}.
\end{aligned} \tag{5.3}$$

The numerical values indicating the relative significance of $\mathscr{R}_0$ are given in Table 3. Some parameters are found to be positive while some are negative. A positive relationship for the parameters implies that an increase in that parameter's values will have a major effect on the frequency of the ailment spread. While a negative relationship means that an increase in the importance of these parameters would help to

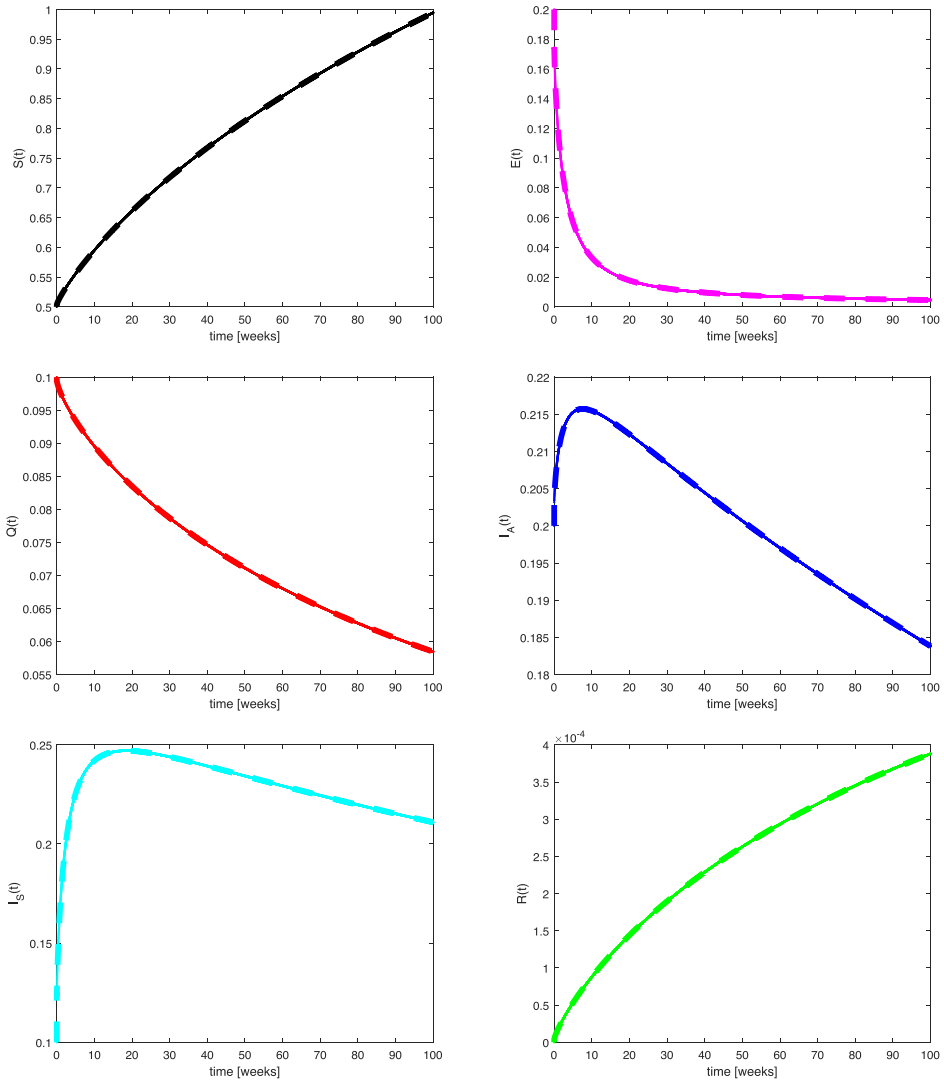

Fig. 5.6. Profiles for behavior of each state variable for the ABC version of the fractional model.

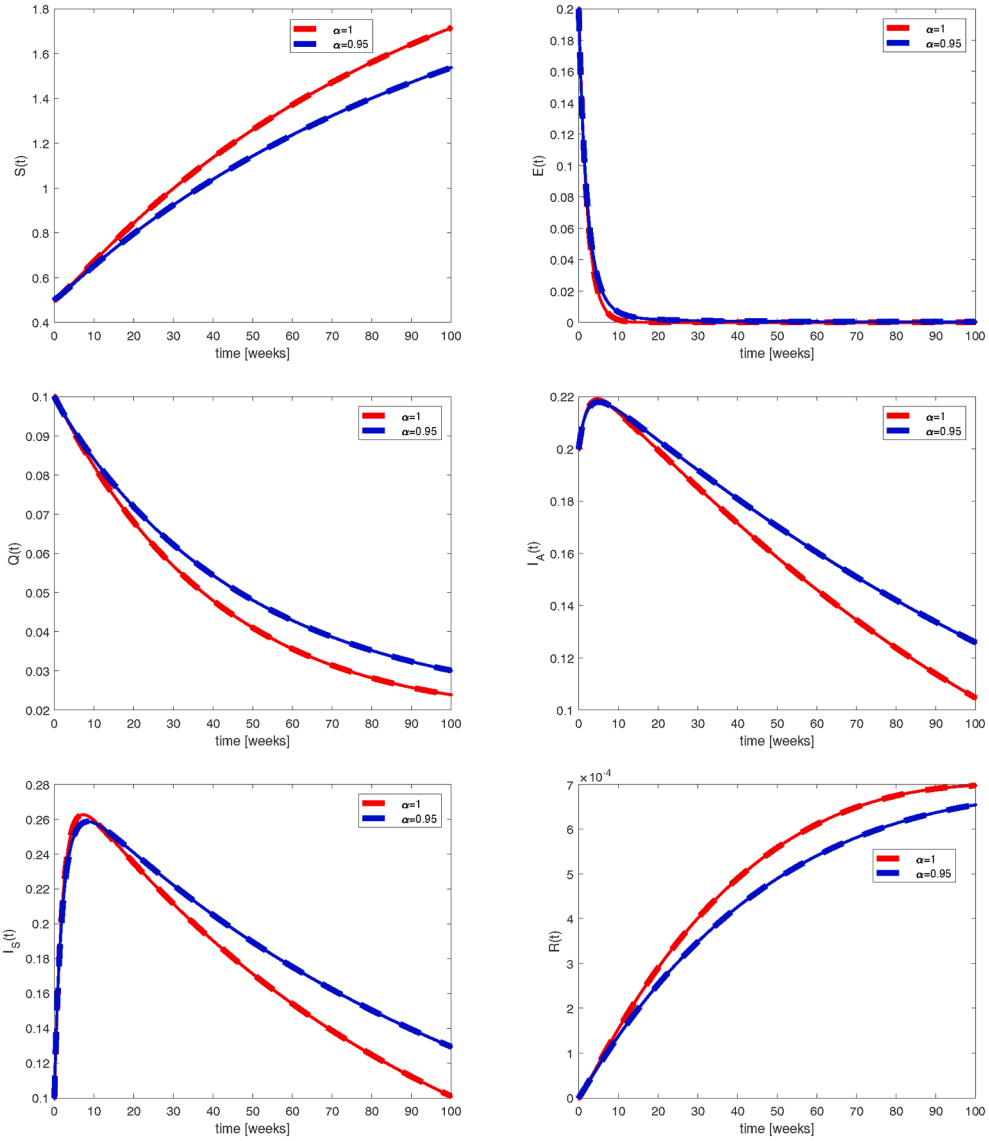

Fig. 5.7. Comparison of each state variables for classical and fractional order.

decrease the violence of the disease. The physical outlook of the numerical signs stated in Table 3 is depicted in Fig. 5.4.

5.2. Numerical simulations

To gain insight into the behavior of the solutions, a numerical solution is needed for both the classical order and the proposed fractional-order model as it involves a nonlinear equation. For this task, we used the recent numerical scheme proposed by Toufik and Atangana in [49]. The numerical scheme for the proposed model (4.4) used in the present analysis is presented by:

$$\begin{aligned} S(t_{k+1}) = S(t_0) \quad & + \frac{1-\alpha}{N(\alpha)} F_1(t_k, S(t_k)) \\ & + \frac{\alpha}{N(\alpha)} \sum_{m=0}^{k} \left[\frac{h^\alpha F_1(t_m, S(t_m))}{\Gamma(\alpha+2)} [(k+1-m)^\alpha (k-m+2+\alpha) \right. \\ & - (k-m)^\alpha (k-m+2+2\alpha)] \\ & - \frac{h^\alpha F_1(u_{m-1}, S(t_{m-1}))}{\Gamma(\alpha+2)} [(k+1-m)^{\alpha+1} \\ & \left. - (k-m)^\alpha (k-m+1+\alpha)] \right]. \end{aligned} \tag{5.4}$$

$$\begin{aligned} E(t_{k+1}) = E(t_0) \quad & + \frac{1-\alpha}{N(\alpha)} F_2(t_k, E(t_k)) \\ & + \frac{\alpha}{N(\alpha)} \sum_{m=0}^{k} \left[\frac{h^\alpha F_2(t_m, E(t_m))}{\Gamma(\alpha+2)} [(k+1-m)^\alpha (k-m+2+\alpha) \right. \\ & - (k-m)^\alpha (k-m+2+2\alpha)] \\ & - \frac{h^\alpha F_2(t_{m-1}, E(t_{m-1}))}{\Gamma(\alpha+2)} [(k+1-m)^{\alpha+1} \\ & \left. - (k-m)^\alpha (k-m+1+\alpha)] \right]. \end{aligned} \tag{5.5}$$

$$\begin{aligned} Q(t_{k+1}) = Q(t_0) \quad & + \frac{1-\alpha}{N(\alpha)} F_3(t_k, Q(t_k)) \\ & + \frac{\alpha}{N(\alpha)} \sum_{m=0}^{k} \left[\frac{h^\alpha F_3(t_m, Q(t_m))}{\Gamma(\alpha+2)} [(k+1-m)^\alpha (k-m+2+\alpha) \right. \\ & - (k-m)^\alpha (k-m+2+2\alpha)] \\ & - \frac{h^\alpha F_3(t_{m-1}, Q(t_{m-1}))}{\Gamma(\alpha+2)} [(k+1-m)^{\alpha+1} \\ & \left. - (k-m)^\alpha (k-m+1+\alpha)] \right]. \end{aligned} \tag{5.6}$$

$$\begin{aligned} I_A(t_{k+1}) = I_A(t_0) \quad & + \frac{1-\alpha}{N(\alpha)} F_4(t_k, I_A(t_k)) \\ & + \frac{\alpha}{N(\alpha)} \sum_{m=0}^{k} \left[\frac{h^\alpha F_4(t_m, I_A(t_m))}{\Gamma(\alpha+2)} [(k+1-m)^\alpha (k-m+2+\alpha) \right. \\ & - (k-m)^\alpha (k-m+2+2\alpha)] \\ & - \frac{h^\alpha F_4(t_{m-1}, I_A(t_{m-1}))}{\Gamma(\alpha+2)} [(k+1-m)^{\alpha+1} \\ & \left. - (k-m)^\alpha (k-m+1+\alpha)] \right]. \end{aligned} \tag{5.7}$$

$$\begin{aligned} I_S(t_{k+1}) = I_S(t_0) \quad & + \frac{1-\alpha}{N(\alpha)} F_5(t_k, I_S(t_k)) \\ & + \frac{\alpha}{N(\alpha)} \sum_{m=0}^{k} \left[\frac{h^\alpha F_5(t_m, I_S(t_m))}{\Gamma(\alpha+2)} [(k+1-m)^\alpha (k-m+2+\alpha) \right. \\ & - (k-m)^\alpha (k-m+2+2\alpha)] \\ & - \frac{h^\alpha F_5(t_{m-1}, I_S(t_{m-1}))}{\Gamma(\alpha+2)} [(k+1-m)^{\alpha+1} \\ & \left. - (k-m)^\alpha (k-m+1+\alpha)] \right]. \end{aligned} \tag{5.8}$$

$$\begin{aligned} R(t_{k+1}) = R(t_0) \quad & + \frac{1-\alpha}{N(\alpha)} F_6(t_k, R(t_k)) \\ & + \frac{\alpha}{N(\alpha)} \sum_{m=0}^{k} \left[\frac{h^\alpha F_6(t_m, R(t_m))}{\Gamma(\alpha+2)} [(k+1-m)^\alpha (k-m+2+\alpha) \right. \\ & - (k-m)^\alpha (k-m+2+2\alpha)] \\ & - \frac{h^\tau F_6(t_{m-1}, R(t_{m-1}))}{\Gamma(\alpha+2)} [(k+1-m)^{\alpha+1} \\ & \left. - (k-m)^\alpha (k-m+1+\alpha)] \right]. \end{aligned} \tag{5.9}$$

To fit the model to the reality of the pandemic, we used the daily cases of the spread of the disease in Nigeria. For this study and for the current situation in the world we are only interested in infected individuals as the week's pass. From Figs. 5.5–5.7, we observed that both population of infected individuals I_S and I_A have been declining as weeks pass which may not be unconnected to existing government restrictions on movement and other contact activities. Not only that, there is a possibility that the government has put in place a public health education system that made the population take safety measures. This further confirmed the result obtained from the fact that a decrease in contact among the population plays a vital role in curtailing the spread of the disease.

The behavior of the system further confirmed the current situation in Nigeria. Both the classical and fractional differential equations indicate that the disease is declining with a very high number of recovery. It is therefore easy to understand that in Nigeria restriction on social contact can work wonders in decreasing the number of infected individuals in addition to quarantine and testing. Meaning it should be of particular interest for all that in the fight against the pandemic is the exposure as a result of contact with infected individuals especially that there those who are asymptomatic (I_A). Equally important, there is also a strong agreement between the classical model and the fractional model as seen in Figs. 5.5 and 5.6.

6. Conclusion

In this current work, we developed a simple mathematical model to investigate the transmission and control of the novel coronavirus disease (COVID-19) from human to human. Principles drawn from the literature of mathematical epidemiology have been used to model how individuals are exposed and infected with the disease and their possible recovery. The mathematical analysis was done using both the ordinary differential equation (ODE) and the fractional differential equation.

It is important for health practitioners and the world at large to understand and predict infected individuals for health concern arrangement of the citizens and to control its spread rate with restricted supply. The data used in the simulation is based on the disease spread in Nigeria. Positivity of the model is established and the basic reproduction number, $\mathscr{R}_0$ is obtained for the model. It is observed that when $\mathscr{R}_0 < 1$ the disease-free equilibrium is locally asymptotically stable otherwise is unstable. The behavior of the system further confirmed the current sit-

uation in Nigeria. Both the classical and fractional differential equations indicate that the disease is declining with a very high number of recovery. It is therefore easy to understand that in Nigeria restriction on social contact can work wonders in decreasing the number of infected individuals in addition to quarantine and testing. Meaning it should be of particular interest for all that in the fight against the pandemic, the exposure as a result of contact with infected individuals especially that there those who are asymptomatic (I_A), be curtail. Equally important, there is also a strong agreement between the classical model and the fractional model as seen in Figs. 5.5 and 5.6. Also the endemic equilibrium E_1 exist and globally stable if $\mathscr{R}_0 > 1$. This means that the disease may persist in society. The sensitivity analysis of $\mathscr{R}_0$ concerning the parameters shows that the most sensitive parameter of our model structure that represents the chance of transmission is the contact rate between susceptible persons and exposed persons. It has the most dominant sensitivity to increase the endemicity of the disease while the rate of transfer of individuals to symptomatic class decreases the endemicity of the disease. Also, using the techniques of fixed point theorems, the existence and uniqueness of solutions are presented.

Furthermore, given that the non-local (fractional order derivatives and integral) operator is better able to predict the future and better fit the experimental data compared to classical order derivatives and integrals, we have generalized the model to a fractional-order model in the sense of the Atangana-Baeanu derivative. Based on the actual data on the number of infected people in Nigeria and the best fitting techniques, we have obtained some of the values of the model's unknown biological parameters, which successfully captured the COVID-19 pattern for the case $\alpha = 1$. Therefore, our results of the ODE form of the model present the situation in Nigeria and with this, we may conclude that authorities and health practitioners in Nigeria need to work hard to ensure that the contact between the exposed individual and susceptible individuals is minimized. This calls for strict social distance and quarantine.

7. Availability of data and materials

All data used in this analysis is provided in the Nigerian center for disease control and Word heath organization, https://ncdc.gov.ng, and https://who.int.

8. Author contributions

The authors contributed equally to this paper. All authors have read and approved the final version of the manuscript.

Declaration of Competing Interest

The authors declare that they have no known competing financial interests or personal relationships that could have appeared to influence the work reported in this paper.

Acknowledgments

The authors acknowledge the financial support provided by the Center of Excellence in Theoretical and Computational Science (TaCS-CoE), KMUTT. The first author was supported by "Petchra Pra Jom Klao Ph.D Research Scholarship from King Mongkut's University of Technology Thonburi" (Grant No. 13/2561). Moreover, the authors express their gratitude for the positive comments received by anonymous reviewers and the editors which have improved the readability and correctness of the paper.

References

[1] Nigeria centre for disease control. covid-19 outbreak in Nigeria: situation report. URL: https://ncdc.gov.ng/diseases/sitreps/?cat=14&name=An%20update%20of%20COVID-19%20outbreak%20 in%20 Nigeria [accessed: 2020-10-14].
[2] World health organization. novel coronavirus diseases 2019. URL: https://www.who.int/emergencies/diseases/novel-coronavirus-2019 [accessed: 2020-10-14].
[3] World health organization. report of the who-china joint mission on coronavirus disease 2019 (covid-19), february 2020. URL: https://www.who.int/docs/defaultsource/coronaviruse/who-china-jointmission-on-covid-19-final-report.pdf [accessed: 2020-10-14].
[4] Abdeljawad T, Hajji MA, Al-Mdallal QM, Jarad F. Analysis of some generalized abc–fractional logistic models. Alexandria Eng J 2020.
[5] Abdo MS, Shah K, Wahash HA, Panchal SK. On a comprehensive model of the novel coronavirus (covid-19) under mittag-leffler derivative. Chaos Solitons Fract 2020: 109867.
[6] Adegboye OA, Adekunle AI, Gayawan E. Early transmission dynamics of novel coronavirus (covid-19) in Nigeria. Int J Environ Res Public Health 2020;17(9): 3054.
[7] Ahmad S, Ullah A, Al-Mdallal QM, Khan H, Shah K, Khan A. Fractional order mathematical modeling of covid-19 transmission. Chaos Solitons Fract 2020;139: 110256.
[8] Ahmed I, Baba IA, Yusuf A, Kumam P, Kumam W. Analysis of caputo fractional-order model for covid-19 with lockdown. Adv Differ Equ 2020;2020(1):1–14.
[9] Ajisegiri W, Odusanya O, Joshi R. Covid-19 outbreak situation in nigeria and the need for effective engagement of community health workers for epidemic response. Global Biosecur 2020;1(4).
[10] Anderson RM, May RM. Helminth infections of humans: mathematical models, population dynamics, and control. In: Advances in parasitology, vol. 24. Elsevier; 1985. p. 1–101.
[11] Asif M, Jan SU, Haider N, Al-Mdallal Q, Abdeljawad T. Numerical modeling of npz and sir models with and without diffusion. Results Phys 2020;19:103512.
[12] Asif M, Khan ZA, Haider N, Al-Mdallal Q. Numerical simulation for solution of seir models by meshless and finite difference methods. Chaos Solitons Fract 2020;141: 110340.
[13] Atangana A. Derivative with a new parameter: theory, methods and applications. Academic Press; 2015.
[14] Atangana A. Fractional operators with constant and variable order with application to geo-hydrology. Academic Press; 2017.
[15] Atangana A. Modelling the spread of covid-19 with new fractal-fractional operators: Can the lockdown save mankind before vaccination? Chaos Solitons Fract 2020;136:109860.
[16] Atangana A, Baleanu D. New fractional derivatives with nonlocal and non-singular kernel: theory and application to heat transfer model. Therm Sci 2016;20(2): 763–9.
[17] Baba IA, Nasidi BA. Fractional order epidemic model for the dynamics of novel covid-19. Alexandria Eng J 2020.
[18] Bailey NT, Sendov B, Tsanev R. Mathematical models in biology and medicine. In IFIP-TC4 working conference on mathematical models in biology and medicine (1972: Varna, Bulgaria). North-Holland Pub. Co.; 1974.
[19] Baleanu D, Jajarmi A, Hajipour M. On the nonlinear dynamical systems within the generalized fractional derivatives with Mittag–Leffler kernel. Nonlinear Dyn 2018; 94(1):397–414.
[20] Baud D, Qi X, Nielsen-Saines K, Musso D, Pomar L, Favre G. Real estimates of mortality following covid-19 infection. Lancet Infect Dis 2020.
[21] Chen S-B, Rashid S, Noor MA, Hammouch Z, Chu Y-M. New fractional approaches for n-polynomial p-convexity with applications in special function theory. Adv Differ Equ 2020;2020(1):1–31.
[22] Danane J, Allali K, Hammouch Z. Mathematical analysis of a fractional differential model of hbv infection with antibody immune response. Chaos Solitons Fract 2020; 136:109787.
[23] Diekmann O, Heesterbeek JAP, Metz JA. On the definition and the computation of the basic reproduction ratio r_0 in models for infectious diseases in heterogeneous populations. J Math Biol 1990;28(4):365–82.
[24] Diethelm K. A fractional calculus based model for the simulation of an outbreak of dengue fever. Nonlinear Dyn 2013;71(4):613–9.
[25] Dourado-Neto D, Teruel D, Reichardt K, Nielsen D, Frizzone J, Bacchi O. Principles of crop modeling and simulation: I. uses of mathematical models in agricultural science. Sci Agricola 1998;55(SPE):46–50.
[26] Edelstein-Keshet L. Mathematical models in biology. SIAM; 2005.
[27] Gomez-Aguilar J, Cordova-Fraga T, Abdeljawad T, Khan A, Khan H. Analysis of fractal-fractional malaria transmission model. Fractals 2020.
[28] Goufo EFD, Khan Y, Chaudhry QA. Hiv and shifting epicenters for covid-19, an alert for some countries. Chaos Solitons Fract 2020;139:110030.
[29] Hajji MA, Al-Mdallal Q. Numerical simulations of a delay model for immune system-tumor interaction. Sultan Qaboos Univ J Sci [SQUJS] 2018;23(1):19–31.
[30] Khan H, Gómez-Aguilar J, Alkhazzan A, Khan A. A fractional order hiv-tb coinfection model with nonsingular Mittag-Leffler law. Math Methods Appl Sci 2020;43(6):3786–806.
[31] Khan MA, Atangana A. Modeling the dynamics of novel coronavirus (2019-ncov) with fractional derivative. Alexandria Eng J 2020.
[32] Kilbas A, Srivastava H, Trujillo J. Theory and applications of fractional derivatial equations. North-Holland Mathematics Studies 2006;204.
[33] Koo JR, Cook AR, Park M, Sun Y, Sun H, Lim JT, Tam C, Dickens BL. Interventions to mitigate early spread of sars-cov-2 in singapore: a modelling study. Lancet Infect Dis 2020.
[34] Linton NM, Kobayashi T, Yang Y, Hayashi K, Akhmetzhanov AR, Jung S-M, Yuan B, Kinoshita R, Nishiura H. Incubation period and other epidemiological characteristics of 2019 novel coronavirus infections with right truncation: a statistical analysis of publicly available case data. J Clin Med 2020;9(2):538.